Acta metall. mater. Vol. 40, No. 4, pp. 795–801, 1992
Printed in Great Britain.

0956-7151/92 $5.00 + 0.00

PREMELTING TRANSITION ON 38°⟨100⟩ TILT GRAIN BOUNDARIES IN (Fe–10 at.% Si)–Zn ALLOYS

B. B. STRAUMAL[1,2], O. I. NOSKOVICH[2], V. N. SEMENOV[2], L. S. SHVINDLERMAN[2], W. GUST[1] and B. PREDEL[1]

[1]Max-Planck-Institut für Metallforschung and Institut für Metallkunde der Universität, Seestr. 75, D-7000 Stuttgart 1, Fed. Rep. Germany and [2]Institute of Solid State Physics, Academy of Sciences of the U.S.S.R., Chernogolovka, Moscow District 142432, Russia

(Received 24 June 1991)

Abstract—Zinc penetration along a 38°⟨100⟩ tilt grain boundary was studied in an Fe–10 at.% Si alloy. For the entire temperature range studied (700–840°C) the grain boundaries are wetted by the melt. A region of accelerated grain boundary diffusion is observed in the single-phase region of the (Fe–10 at.% Si)–Zn diagram below the critical temperature $T_{cr} = 790 \pm 5$°C. At a concentration C_{bt} the product of the segregation factor, the thickness and the diffusion coefficient of the grain boundary, $s\delta D_b$, abruptly falls to a "normal" value. Above T_{cr} no discontinuities in $s\delta D_b$ are observed. A singularity is observed in the $C_{bt}(T)$ curve at the peritectic temperature T_{per}. The data obtained confirm the previously proposed model of a grain boundary premelting transition. This model explains in particular, why there are no singularities in the $C_{bt}(T)$ curve of the alloy studied below T_{per}. This feature distinguishes the Fe–10 at.% Si alloy from the previously studied Fe–Si alloys containing 5, 6 and 12 at.% Si, which undergo a bulk magnetic or concentrational ordering transition.

Résumé—On a étudié la pénétration du zink aux joint des grains de la pente 38°⟨100⟩ dans le bicrystall d'alliage Fe–10 at.% Si à l'intervalle des températures de 700 à 840°C. Dans la toute intervalle des températures étudié a lieu la humectation des joints des grains avec l'alliage fondu. Dans le domaine homophase de diagramme de phase (Fe–10 at.% Si)–Zn à $T < T_{cr}$ ($T_{cr} = 790 \pm 5$°C) la region de la diffusion intergranulaire anomalement rapide se trouve plus profondement que couche intergranulaire humectée. A la certaine concentration C_{bt} le produit de coefficient de segregation s, de grosseur du joint δ et de coefficient de diffusion intergranulaire D_b se varie par le saut. A $C < C_{bt}$ se trouve la région de diffusion intergranulaire "normale". La ligne $C_{bt}(T)$ sur la diagramme de phase se termine à $T_{cr} = 790 \pm 5$°C. A la température peritectique T_{per} sur la ligne $C_{bt}(T)$ une saillie a lieu. Tout l'ensemble des donnés observés on peut expliquer par la modèle thermodinamique sur la transformation du phase de la préfusion aux joints des grains. Cette modèle explique en particulier parquoi à $T < T_{per}$ la ligne $C_{bt}(T)$ dans l'alliage etudié n'a pas aucune singularités analogue de celles-même à l'alliages Fe–5 at.% Si, Fe–6 at.% Si et Fe–12 at.% Si, ou les transformations de phase de la mise en ordre magnétique et chimique en volume ont lieu.

Zusammenfassung—Es wurde das Eindringen von Zn in eine 38°⟨100⟩-Kippkorngrenze eines Fe–10 At.% Si-Zweikristalls untersucht. Im untersuchten Temperaturbereich von 700 bis 840°C wurde die Benetzung der Korngrenze durch die Schmelze beobachtet. Im einphasigen Bereich des Zustandsdiagramms (Fe–10 At.% Si)–Zn wurde bei $T < T_{cr}$ ($T_{cr} = 790 \pm 5$°C) an der Korngrenze ein Abschnitt beschleunigter Diffusion beobachtet. Bei der Konzentration $C_{bt}(T)$ fällt das Produkt aus dem Segregationsfaktor s, der Korngrenzendicke δ und dem Korngrenzendiffusionskoeffizienten D_b sprunghaft auf eine "normale" Größe ab.Bei $T > T_{cr}$ gibt es keine sprunghafte Änderung von $s\delta D_b$. Bei der peritektischen Temperatur T_{per} weist der $C_{bt}(T)$-Verlauf eine Besonderheit auf. Alle beobachteten Erscheinungen bestätigen die früher vorgeschlagene Hypothese über einen Korngrenzenphasenübergang des Vorschmelzens. Diese Hypothese erklärt z.B., warum bei der untersuchten Legierung für $T < T_{per}$ der $C_{bt}(T)$-Vorlauf keine Besonderheiten aufweist. Damit unterscheidet sich diese Legierung von den früher untersuchten Fe–Si–Legierungen mit 5, 6 und 12 At.% Si, wo entweder ein magnetischer oder chemischer Ordnungsübergan im Volumen des Kristalls auftritt.

1. INTRODUCTION

In their previous works the authors studied zinc penetration along [100] tilt grain boundaries in bicrystals of the following body-centered cubic (b.c.c.) alloys: Fe–5 at.% Si [1], Fe–6 at.% Si [2] and Fe–12 at.% Si [3]. The Fe–5 at.% Si and Fe–6 at.% Si alloys undergo a magnetic ordering at ~730°C. Here the α phase is transformed from a paramagnetic state into a ferromagnetic one [4, 5]. The Fe–12 at.% Si alloy undergoes a "chemical" ordering instead of a magnetic one. The high-temperature disordered b.c.c. A2 phase is transformed into an ordered B2 phase at 800°C [4, 5].

It was shown [3] that a wetting transition occurs at $T_W = 794 \pm 4$°C during zinc penetration along grain boundaries. This means that the contact angle θ at the site of grain boundary intersection with the

sample surface covered with a zinc layer has a non-zero value below the wetting temperature T_W [Fig. 1(a)]. At $T = T_W$ the contact angle θ decreases from 180°C to zero rapidly, its value being zero at $T > T_W$ [Fig. 1(b)]. A similar wetting transition has previously been observed in other systems, namely, Zn–Sn [6, 7], Al–Zn [8–10], Al–Pb [8] and Ag–Pb [11]. For the Fe–5 at.% Si alloy the contact angle θ is equal to zero over the whole temperature range (650–950°C) studied [1]; however, when the pressure is raised [2], wetting disappears at $P_W = 0.5$ GPa. Above P_W the contact angle θ is non-zero. As was shown in [12], the wetting pressure P_W depends on temperature. In the experiments described in [1–3, 12] the thickness of the zinc layer applied to the surface was selected in such a way that the wetting interlayer penetrated along the grain boundaries to a depth of $l = 50$–$200\ \mu$m from the surface [see Fig. 1(b)]. By studying the zinc distribution in a sample below this interlayer, one can determine the diffusion characteristics of the grain boundaries. Figure 1(c) schematically shows the zinc distribution in a bicrystal after a diffusion anneal. Here, C_s is the zinc solubility limit in an Fe–Si alloy at the annealing temperature. C_s is determined by the solidus line above the peritectic temperature T_{per} and by the solvus line below it.

It was found that there exists a region on the grain boundary (directly below the wetting interlayer) in which the rate of zinc diffusion is two orders of magnitude higher than usual. Zinc concentrations for which such a permeability increase is observed range from C_s to C_{bt}. At the concentration C_{bt} the value of the grain boundary diffusivity, $s\delta D_b$, abruptly decreases (here s is the grain boundary segregation factor, δ is the grain boundary diffusional thickness and D_b is the grain boundary diffusion coefficient). Below C_{bt} the values of $s\delta D_b$ are close to those characteristic for grain boundaries in iron and its alloys [13]. The depth of zinc penetration in the concentration range from C_s to C_{bt} was shown to be proportional to $t^{1/4}$, t being the annealing time [1]. This means that, although zinc penetrates with a rate two orders of magnitude greater than normal at concentrations below C_{bt}, the diffusional process is still similar to that occurring at concentrations below C_{bt}. It was also found that the concentration C_{bt}, at which the abrupt change of $s\delta D_b$ occurs, depends strongly on the annealing temperature.

The temperature dependence of the concentrations C_{bt} is presented in Fig. 5(c) and (e) along with solidus and solvus lines $C_s(T)$. In the Fe–5 at.% Si alloy the discontinuity in $s\delta D_b$ at concentration C_{bt}, as well as wetting, is observed over the whole temperature range (650–950°C) studied [Fig. 5(c)] [1]. When the pressure exceeds P_W, the region of rapid diffusion disappears simultaneously with grain boundary wetting [2]. In the Fe–12 at.% Si alloy the region of rapid grain boundary diffusion disappears at $T < T_W$ ($T_W = 749 \pm 4$°C) also simultaneously with wetting [Fig. 5(e)]. In contrast to the (Fe–5 at.% Si)–Zn

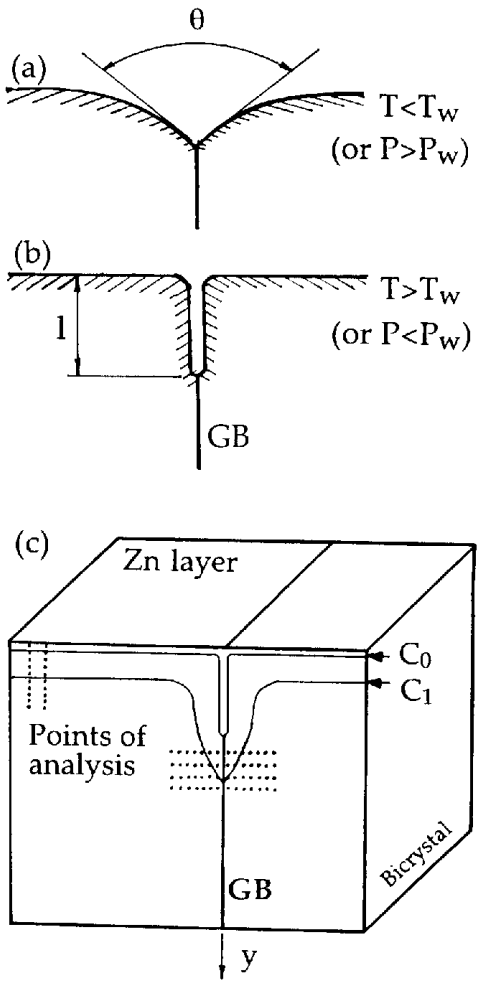

Fig. 1. (a) The contact angle θ at the site of the grain boundary (GB) intersection with the zinc covered sample surface for $T < T_W$ and $\theta = 0$. (b) The same as (a), but for $T > T_W$ and $\theta = 0$. (c) Schematic diagram showing zinc concentration isotherms in an Fe–10 at.% Si bicrystal after anneal.

alloys the $C_{bt}(T)$ line for the (Fe–12 at.% Si)–Zn alloys is bounded by a critical point at temperature $T_{cr} = 801 \pm 2$°C. Above T_{cr} the abrupt change of grain boundary diffusion coefficient gradually becomes "diffuse". At temperatures above ~870°C the diffusion profiles do not contain a region of rapid diffusion at all.

There exists a number of theoretical works in which the phase transitions on interfaces accompanying wetting are predicted [14–16]. Such transitions include premelting, prewetting, layering, etc. They are related to the formation of a thermodynamically stable thin liquid (quasi-liquid) interlayer on interfaces. In the system Fe–Si–Zn an abrupt change in the properties of grain boundaries occurs at concentration C_{bt}. It is assumed to be a premelting transition. In this case the increase of $s\delta D_b$ may be explained by the formation of a quasi-liquid interlayer on the grain boundary, for which the diffusional thickness of the interface δ is increased by approximately a factor of 100. All of the necessary conditions for a premelting transition to occur are satisfied by the system. These are (1) a high positive value of

the enthalpy of mixing of the solution components, (2) a wetting of grain boundaries in the two-phase region "solid-melt", and (3) the fact that the phenomena mentioned are observed on grain boundaries of the component having the higher melting temperature (iron). Therefore, it is quite reasonable to say that a premelting transition is observed on grain boundaries.

The temperature dependence of $C_{bt}(T)$ presented in Fig. 5(c) and (e) contain singularities of the following three different types:

1. At temperatures close to bulk ordering (magnetic [1] and concentrational [3]), the lines $C_{bt}(T)$ have protuberances directed towards lower concentrations.
2. Ordering leads to the disappearance of the region of rapid grain boundary diffusion. At temperatures below the Curie point, the $C_{bt}(T)$ line nearly merges with the C_s line. At temperatures below the A2–B2 ordering point the region of rapid grain boundary diffusion disappears simultaneously with wetting.
3. At $T = T_{per}$ the zinc solubility C_s in the Fe–5 at.% Si alloy increases abruptly, while C_{bt} decreases nearly to zero. [In the Fe–10 at.% Si alloy the zinc solubility C_s changes slightly with temperature near T_{per}, and the $C_{bt}(T)$ line singularity in the vicinity of T_{per} is nearly undistinguishable.]

The hypothesis of a grain boundary premelting transition at the concentration C_{bt} provides a basis for interpreting all of the variations observed for $C_{bt}(T)$. The aim of the present paper was to find experimental answers to the following questions:

1. Is it true that the protuberances directed towards lower concentrations on the $C_{bt}(T)$ curves are caused by bulk magnetic or concentration ordering?
2. Is it true that bulk ordering "suppresses" the grain boundary premelting transition and leads to the disappearance of the region of rapid grain boundary diffusion?
3. Is it true that C_{bt} increases as C_s decreases and vice versa for the disordered phase?

2. EXPERIMENTAL

The above questions can be answered by investigation of zinc grain boundary penetration into an Fe–10 at.% Si alloy. Above 700°C this alloy does not undergo either magnetic or concentrational ordering, which are assumed [1, 3] to cause the appearance of the discontinuity in the $C_{bt}(T)$ line. At the same time the alloy can be expected to exhibit stronger changes in C_s in the vicinity of T_{per} than those exhibited by the Fe–12 at.% Si alloy [4, 5]; see also Fig. 5(a) and (b). To demonstrate this, an Fe–10 at.% Si bicrystal having a 38°⟨100⟩ tilt grain boundary (where the tilt angle is measured between {100} planes) and a diameter of 10 mm was grown by the electron beam zone melting method. The silicon concentration at various locations in the bicrystal ranged from 9.9 to 10.1 at.%. Samples 6–10 mm long and 1.5 mm × 1.5 mm in cross-section were cut from the bicrystal by spark erosion in such a way that the grain boundary was located in the middle of the sample, perpendicular to its length. A zinc layer was applied to the samples by immersion in a Zn melt. Before immersion the samples were mechanically ground and chemically polished in a solution consisting of 80% H_2O_2, 14% H_2O and 6% HF (by volume). After application of zinc the applied zinc layer was completely removed from two opposite sides of the samples. From the other two sides, the excess of zinc was partially removed so that only a 100–150 μm thick layer remained.

The samples prepared as described above were sealed in evacuated silica ampoules and annealed in a furnace in the temperature range 700–840°C with the temperature being maintained within ±0.5°C. After annealing, the samples were embedded in a holder using Wood's metal and then mechanically ground and polished. The polished surface of the samples were etched for 10–15 s to reveal the grain boundaries. The site of grain boundary intersection with the sample surface was marked with Vickers microhardness indentations, after which the sample was mechanically repolished in such a way that the traces of chemical etching were removed, but the microhardness indentations remained. The zinc concentration profiles across the boundary were then determined by means of electron microprobe analysis [see Fig. 1(c)]. The Zn and Si concentrations were determined from the intensities of the characteristic X-rays from Zn and Si with the necessary corrections associated with the standard methods of quantitative electron probe microanalysis being made [17].

In order to determine bulk zinc solubilities C_s the zinc concentration profiles in the bulk diffusion layers far from the grain boundary and perpendicular to the sample surface were determined [Fig. 1(c)]. The concentration C_{bt} was determined from lateral concentration profiles measured parallel to the sample surface to which the zinc had been applied [Fig. 1(b)]. In previous studies the bulk and grain boundary diffusion profiles were measured continuously, that is, the sample was moved continuously under the electron beam. In the present work the measurements were performed using JEOL-6400 instrument, in which the sample could be positioned with an accuracy of 1 μm and the concentration profile could be determined using a point-by-point method. In order to determine precisely the coordinates of the grain boundary or the diffusion zone border, concentration profiles were first determined by meauring zinc contents at 5–10 μm intervals using a short counting time at each point. Later, the area of interest was scanned with 1 μm steps and longer counting times. In addition to the intensity of the Zn-K_α and Si-K_α X-ray lines the microprobe current and background

to the left and right of the lines were measured. The concentration profiles measured on a cross-section, perpendicular to the grain boundary plane [see Fig. 1(c)], are symmetrical about the grain boundary plane reaching a maximum of C_b on the boundary. The distance between diffusion profiles along the grain boundary was usually 2–5 mm.

3. RESULTS AND DISCUSSION

Figure 2 shows the dependences of the concentrations C_b upon depth y plotted in so-called Fisher's coordinates ($\log C_b$ vs y). If Fisher's model [18] is valid, the slope of a diffusion profile in these coordinates is proportional to the grain boundary diffusivity $s\delta D_b$. Each of the first five diffusion profiles $C_b(y)$ contain two distinct linear regions. They intersect at concentration C_{bt}. In the concentration range from C_s to C_{bt} the slope of the lines is small (large $s\delta D_b$). At concentration C_{bt}, the profiles have a knee. The region with large slope (small $s\delta D_b$) corresponds to $C < C_{bt}$. At $T > 790$°C, the knee on $C_{bt}(T)$ curves becomes diffuse. However, some vestiges of the high and low slope regions on the $C_b(y)$ curves are preserved at $T > T_{cr}$ in the temperature interval about 50–70°C. At the highest temperature interval studied the diffusion profiles $C_b(y)$ contain only the large slope region.

Figure 3 presents the (Fe–10 at.% Si)–Zn phase diagram. The plot contains two lines, the zinc bulk solubility limit $C_s(T)$ and the $C_{bt}(T)$ line. $C_s(T)$ is a solidus line at $T > T_{per}$, while at $T < T_{per}$ it is a solvus line [see Fig. 4(d)]. $C_s(T)$ contains a characteristic singularity at $T = T_{per.}$. At this point C_s reaches its maximum, while the $C_{bt}(T)$ line reaches its minimum at the same temperature. Above $T = 790$°C the C_{bt} line comes to an end, because the sharp transition of the slope on the $C_b(y)$ profiles disappears. At temperatures below T_{per} the C_{bt} curves do not contain any singularities down to $T = 700$°C. On the whole the curves $C_s(T)$ and $C_{bt}(T)$ seem to be inverted with respect to each other, that is C_{bt} decreases as C_s increases and vice versa.

The grain boundary wetting phenomena can be described using the equation for the wetting layer excess energy Ω [14, 15]

$$\Omega = 2\sigma_{CF} + l \cdot \Delta g + V(l). \qquad (1)$$

Here, σ_{CF} is the surface energy of the "crystal-wetting phase" interface, l is the thickness of a wetting layer, Δg is the excess free energy of the wetting layer, and

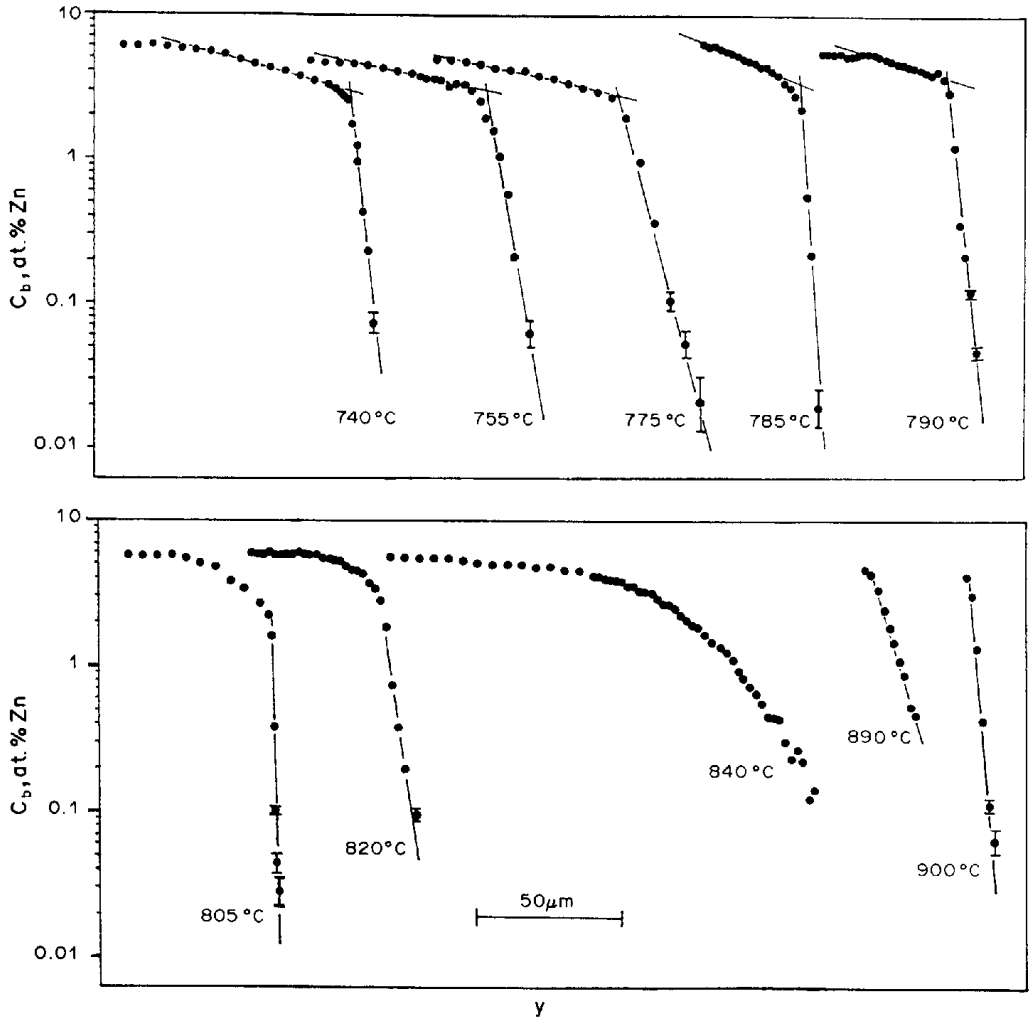

Fig. 2. The dependencies of grain boundary Zn concentration C_b upon depth y for various temperatures.

$V(l)$ is the free energy of interaction of the "crystal-wetting phase" interfaces.

A grain boundary is replaced by a wetting interlayer, if the grain boundary surface tension σ_{GB} is no less than the free energy of a wetting interlayer, i.e. if

$$\sigma_{GB} > \Omega. \tag{2}$$

Figure 4 shows a hypothetical phase diagram with a miscibility gap, a horizontal line for a wetting transition at T_w in the two-phase region, and a line for a premelting transition in the single-phase region. Also, the dependences of σ_{GB} and Ω on l are sketched in this figure. If the alloy composition is changed from the left to the right side of the phase diagram, Δg will decrease and ultimately approach zero at the boundary of the single-phase region for constant T greater than T_w [see Fig. 4(e)]. The equilibrium thickness of the wetting interlayer at a grain boundary is determined by the minimum of the Ω function. If $\Omega > \sigma_{GB}$, no interlayers are observed at the grain boundary [Fig. 4(a)]. When $\Omega = \sigma_{GB}$, the $\Omega(l)$ curve contacts the σ_{GB} line at a point l_0 [Fig. 4(b)]. Here, a premelting transition occurs, and a layer of the wetting phase of thickness l_0 is formed at a grain boundary. Further, as $\Delta g \to 0$, l_0 increases. At the boundary of the single-phase region $C = C_s$ and the excess energy of the wetting phase Δg approaches zero, while l_0 goes into infinity. This means complete wetting.

Complete wetting can be observed only if the following two conditions are satisfied: (1) $2\sigma_{SL} + V(\infty) < \sigma_{CF}$ and (2) $V(l)$ has a global minimum at the point $l(\infty)$. The second condition means that

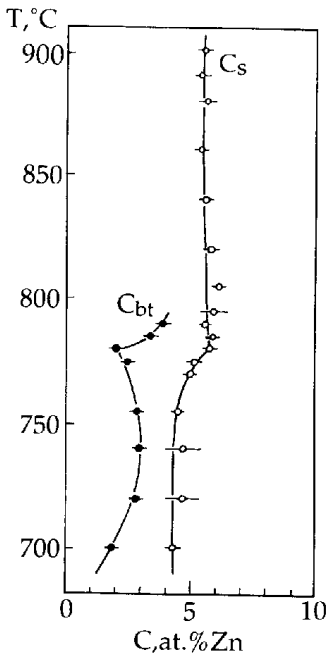

Fig. 3. The (Fe–10 at.% Si)–Zn phase diagram showing the solubility limit $C_s(T)$ (solidus and solvus) and grain boundary transition line $C_{bt}(T)$.

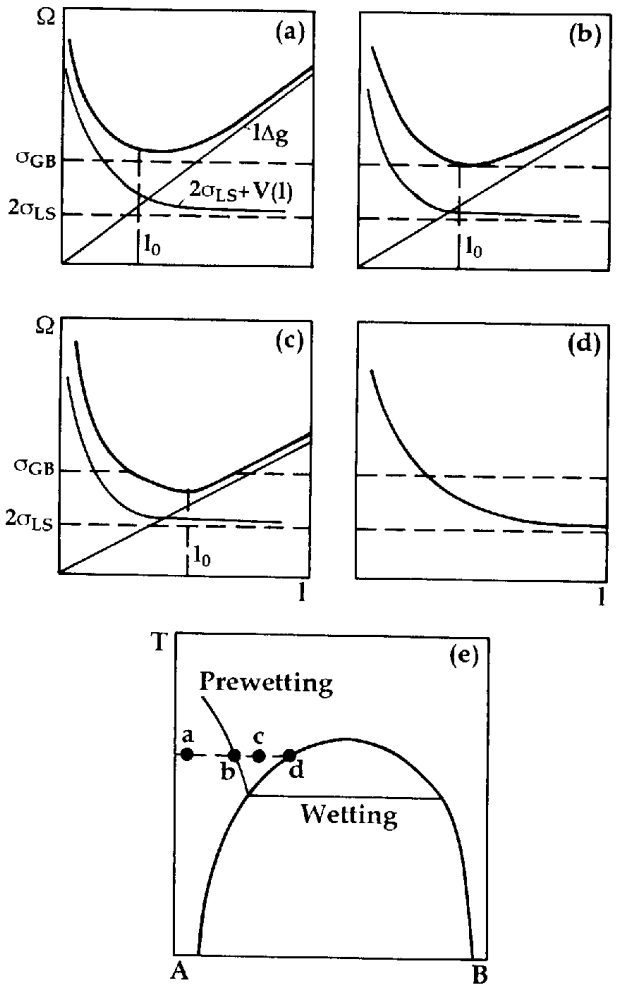

Fig. 4. The dependencies of the wetting layer excess energy Ω on its thickness l. σ_{CF} is the surface energy of the "crystal-wetting phase" interface, l is the thickness of a wetting layer, Δg is excess free energy of the wetting layer, $V(l)$ is the free energy of interaction of the "crystal-wetting phase" interfaces, and σ_{GB} is a grain boundary surface tension. The sum of the hyperbola $V(l)$, straight line $l\Delta g$, and $2\sigma_{CF}$ gives Ω. (a–d) Δg gradually decreases in going from (a) to (d). (e) Schematic diagram of a hypothetical phase diagram of A and B with a miscibility gap showing a boundary line between the wetting and prewetting regimes. The points a–d correspond to Fig. 4(a)–(d).

"crystal-wetting phase" interfaces must repel each other.

Let V have a power law dependence on l. Then

$$V(l) = w/l^n. \tag{3}$$

If the grain boundary concentration C_b equals the bulk solubility limit C_s, i.e. the point of interest belongs to either the solvus or solidus line, then $\Delta g = 0$. Expanding Δg into a power series in terms of $(C_s - C_b)$ for small deviations of C_s and truncating the series after the first term, one obtains

$$\Delta g = b(C_s - C_b). \tag{4}$$

The Ω function, derived from equations (1), (3) and (4), reaches its minimum $\Omega(l_0)$ at

$$l_0 = [b(C_s - C_b)/nw]^{-1/(n+1)}. \tag{5}$$

Thus,

$$\Omega(l_0) = \Omega_0 = 2\sigma_{CF} + (nw)^{1/(n+1)} \times b(C_s - C_b)^{n/(n+1)}(1 + n^{-1}). \quad (6)$$

When the condition $\Omega_0 = \sigma_{GB}$ is met, a premelting transition occurs. In this transition the grain boundary is replaced by an interlayer of a zinc-enriched phase. From this condition we obtain

$$C_{bt} = C_s - \frac{(\sigma_{GB} - 2\sigma_{CF})^{(n+1)/n}}{b(wn)^{-n}(1 + n^{-1})^{(n+1)/n}}. \quad (7)$$

Equation (7) relates the premelting transition concentration C_{bt} to the solubility limit C_s. However, σ_{GB} and σ_{CF} also depend upon the concentration C. Therefore, experimental observations cannot be interpreted in a straightforward way using equation (7). Indirectly, the validity of this equation is confirmed by the following facts. In the Fe–Zn system (see Fig. 5(b) and [4, 5]) the peritectic line nearly passes through the tip of the miscibility gap. It is known that $\sigma_{CF} \to 0$ as the tip of the gap is approached. According to equation (7) this must lead to a decrease in C_{bt}. This very behavior of the $C_{bt}(T)$ line was observed in [1]. Comparing the shapes of the $C_s(T)$ lines in Fig. 5(b) to (c) we see that the higher the silicon content, the smaller the change in C_s near T_{per}. Accordingly, the shape of the $C_{bt}(T)$ line is changed. While C_{bt} in the (Fe–5 at.% Si)–Zn system falls nearly to zero as $T \to T_{per}$, this decrease of C_{bt}

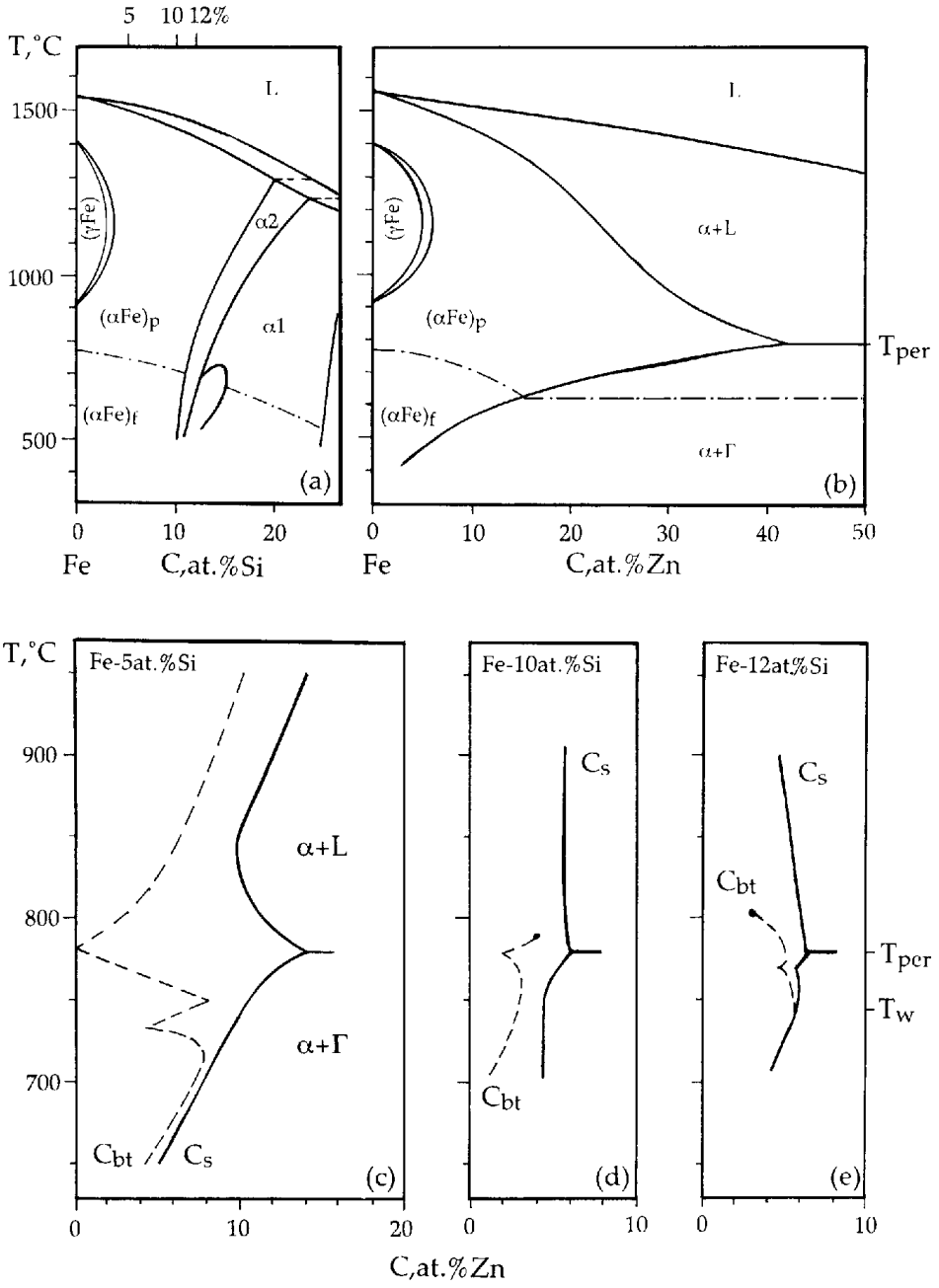

Fig. 5. (a) Fe-rich end of the Fe–Si phase diagram [5]. (b) Fe-rich end of the Fe–Zn phase diagram [5]. (c) (Fe–5 at.% Si)–Zn phase diagram. (d) (Fe–10 at.% Si)–Zn phase diagram. (e) (Fe–12 at.% Si)–Zn phase diagram. The dotted lines on the diagrams (c)–(e) are $C_{bt}(T)$ lines for the grain boundary premelting phase transition.

is small in the (Fe–10 at.% Si)–Zn system. Finally, no decrease in C_{bt} at $T = T_{per}$ is observed for the (Fe–12 at.% Si)–Zn system. The increase in C_{bt} near T_{per} is also very small. Thus, equation (7) satisfactorily describes in a qualitative way changes in the shapes of $C_s(T)$ and $C_{bt}(T)$ lines caused by an increase in the silicon content in the (Fe–Si)–Zn system.

At temperatures far from T_{per} in the (Fe–10 at.% Si)–Zn system C_s and C_{bt} change smoothly. This, again, is in agreement with equation (7). This is distinctive for the Fe–10 at.% Si alloy as compared to the Fe–5 at.% Si and Fe–12 at.% Si alloys, for which magnetic and concentrational ordering are observed. In these alloys, $V(l)$ is no longer described by equation (3). As was shown previously [1, 3], below the ordering (magnetic [1] or concentrational [3]) temperature there appears to be an attraction between the "halves" of the bicrystal separated by a layer of thickness l_0. If the attraction between "crystal-wetting phase" interfaces is strong enough, the function $V(l)$ will no longer have a global minimum at $l \to l(\infty)$. This may lead to a decrease in the concentration range of existence of the premelted phase on a grain boundary [as observed for the (Fe–5 at.% Si)–Zn system [1], Fig. 5(c)], or even a transition from complete to incomplete wetting of grain boundaries may occur [as observed for the (Fe–12 at.% Si)–Zn system [3], Fig. 5(e)]. Such a type of system behavior is not described by the approximate equation (7).

Comparing Figs 5(c), (d) and (e) it can be seen that the disappearance of grain boundary premelting and prewetting in the systems (Fe–5 at.% Si)–Zn and (Fe–12 at. Si)–Zn is really caused by the bulk ordering. The only difference between the Fe–10 at.% Si alloy and the Fe–5 at.% Si and Fe–12 at.% Si alloys is the absence of an ordering transition in the temperature range from 700 to 800°C. It can also be seen that grain boundary premelting and wetting transitions really do not disappear with temperature decrease in the Fe–10 at.% Si alloy.

4. CONCLUSIONS

From the results of our experimental study we can conclude the following.

1. Grain boundary wetting by a zinc-based melt during zinc penetration of 38°⟨100⟩ tilt boundaries in an Fe–10 at.% Si alloy is observed over the entire temperature range (700–840°C) studied.

2. In the range from the lowest temperature studied (700°C) up to $T_{cr} = 790 \pm 5$°C a region of accelerated diffusion is observed on grain boundaries in the concentration range from C_s (bulk solubility limit for zinc) to C_{bt}. At concentration C_{bt} the rate of zinc grain boundary diffusion abruptly decreases to typical values for grain boundary diffusion in iron. At C_{bt} a knee is observed in curves of grain boundary zinc penetration. We explain the existence of a region of rapid grain boundary diffusion in terms of a premelting transition and the formation of a thin equilibrium layer of a liquid or quasi-liquid phase.

3. The above mentioned knee disappears at $T_{cr} = 790 \pm 5$°C, but certain features of rapid grain boundary diffusion are also observed at higher temperatures.

4. At T_{per} C_{bt} reaches its minimum. At the same temperature the bulk zinc solubility is maximal. In contrast to the previously studied ordering Fe–Si alloys the $C_{bt}(T)$ line for the alloy in this study does not have any singularities below T_{per}. Also the regions of accelerated grain boundary diffusion and wetting do not disappear.

5. Thus, the singularities in the $C_{bt}(T)$ curve related to the miscibility gap and bulk ordering can also be observed separately. This further supports the hypothesis of the grain boundary premelting proposed in [1–3] as an approach of explaining the accelerated zinc diffusion along grain boundaries in Fe–Si alloys.

Acknowledgements—The authors are grateful to Professor R. A. Fournelle, Professor Ch. Herzig and Dr. E. Rabkin for fruitful discussions of the results, and to Dr. E. Bischoff and Miss A. Holme for their help in operating the electron probe microanalyzer. One of the authors (B.B.S.) is also grateful to the Alexander von Humboldt Foundation for financial support of his work in Stuttgart.

REFERENCES

1. E. I. Rabkin, V. N. Semenov, L. S. Shvindlerman and B. B. Straumal, *Acta metall. mater.* **39,** 627 (1991).
2. L. S. Shvindlerman, W. Łojkowski, E. I. Rabkin and B. B. Straumal, *C. Physique*, Coll. C1 **51,** 629 (1990).
3. O. I. Noskovich, E. I. Rabkin, V. N. Semenov, B. B. Straumal and L. S. Shvindlerman, *Acta metall. mater.* **39,** 3091 (1991).
4. O. Kubaschewski, *Iron–Binary Phase Diagrams*, p. 79. Springer, Berlin (1982).
5. T. B. Massalski *et al.* (editors), *Binary Alloy Phase Diagrams*, p. 1108. Am. Soc. Metals, Metals Park, Ohio (1986).
6. A. Passerone, N. Eustatopoulos and P. Desre, *J. less-common Metals* **52,** 37 (1977).
7. A. Passerone and R. Sangiorgi, *Acta metall.* **33,** 771 (1985).
8. K. K. Ikeuye and C. S. Smith, *Trans. Am. Inst. Min. Engrs* **185,** 762 (1949).
9. N. Eustatopoulos, L. Coudurier, J. C. Joud and P. Desre, *J. Cryst. Growth* **33,** 105 (1976).
10. J. H. Rogerson and J. C. Borland, *Trans. Am. Inst. Min. Engrs* **227,** 2 (1963).
11. A. Passerone, R. Sangiorgi and N. Eustatopoulos, *Scripta metall.* **16,** 547 (1982).
12. W. Łojkowski, E. Rabkin, J. Swiderski and V. Paidar, *Scripta metall. mater.* To be published.
13. I. Kaur, W. Gust and L. Kozman, *Handbook of Grain and Interphase Boundary Diffusion Data*, p. 857. Ziegler Press, Stuttgart (1989).
14. P. G. de Gennes, *Rev. Mod. Phys.* **57,** 827 (1985).
15. S. Dietrich, in *Phase Transitions and Critical Phenomena* (edited by C. Domb and J. Lebowitz), Vol. 12, p. 1. Academic Press, New York (1988).
16. R. Kikuchi and J. W. Cahn, *Phys. Rev. B* **36,** 418 (1987).
17. S. J. B. Reed, *Electron Microprobe Analysis*, p. 285. Cambridge Univ. Press (1975).